Journal of Applied Electrochemistry (2006) 36:1133–1141
DOI 10.1007/s10800-006-9198-8

Scale-up of the perforated bipole trickle-bed electrochemical reactor for the generation of alkaline peroxide

NEERAJ GUPTA* and C.W. OLOMAN
Department of Chemical & Biological Engineering, University of British Columbia, Vancouver, BC, V6T1Z4, Canada
*(*author for correspondence, Fax: +1-613-991-2384, E-mail: neeraj.gupta@nrc-cnrc.gc.ca)*

Received 27 December 2005; accepted in revised form 26 June 2006

Key words: 3D electrodes, electrochemical, Electroreduction, electrosynthesis, graphite felt, oxygen, peroxide, trickle-bed

Abstract

This paper reports work on the scale-up of a perforated bipole trickle-bed electrochemical reactor for the electro-synthesis of alkaline peroxide. The reactor uses a relatively simple cell configuration in which a single electrolyte flows with oxygen gas in a flow-by graphite felt cathode, sandwiched between a microporous polyolefin diaphragm and a nickel mesh/perforated Grafoil anode/bipole. Both one and two-cell reactors are scaled-up from cathode dimensions 120 mm high by 25 mm wide and 3.2 mm thick (reactor-A) to 630 mm high by 40 mm wide and 3.2 mm thick (reactor-B). The scale-up is achieved by the use of constrictions that prevent segregation of the 2-phase flow in the larger cell, combined with switching from a polypropylene to a polyethylene diaphragm with improved transport properties and raising the electrolyte feed concentration from 1 to 2 M NaOH.For the one-cell reactor-B with a polypropylene diaphragm, operating on a feed of 1 M NaOH and oxygen at 900 kPa(abs)/20 °C, the peroxide current efficiency at a superficial current density of 5 kA m^{-2} increases from 27% (un-constricted cathode) to 57% with a constricted cathode. The corresponding current efficiencies at 3–5 kAm^{-2} for reactor-A and the constricted reactor-B are respectively 69–64% and 66–57%. Under similar conditions at 3–5 kA m^{-2} the one-cell constricted reactor-B with a polyethylene diaphragm gives current efficiencies of 88–64%, and changing to an electrolyte of 2 M NaOH raises this range to 90–80%. At 3–5 kA m^{-2} the equivalent two-cell (bipolar) constricted reactor-B shows current efficiencies of 82–74% and at 5 kA m^{-2} obtains 0.6 M peroxide in 2 M NaOH with specific energy 6.5 kWh per kg H_2O_2.

Nomenclature

i	Current density A m^{-2}
κ	Electrolyte (solution) conductivity S m^{-1}
L	Characteristic length m
V	Electrode potential V
Wa	Wagner number (ratio of Faradaic to Ohmic resistance) dimensionless

1. Introduction

Hydrogen peroxide is one of the most important chemicals used for bleaching and brightening wood pulps. The relevance of peroxide has grown over the last decade due to environmental restrictions imposed on chlorine based chemicals, such that many pulp and paper mills now consume 5–10 tonne day^{-1} of hydrogen peroxide.

Over 90% of H_2O_2 is now manufactured by the conventional thermochemical catalytic auto-oxidation of anthra-quinols in a capital intensive process at dedicated plants with capacities above 50 tonne day^{-1} [1]. As pulp mills are scattered across the world, an onsite process for hydrogen peroxide generation at rates up to 10 tonne day^{-1} would give the pulp and paper industry operating flexibility and eliminate the need for hydrogen peroxide transportation and storage. For most applications, the pulp and paper industry uses alkaline peroxide in dilute solutions (ca. $3\%_w$ H_2O_2), such as can be obtained by the electro-reduction of oxygen [2]. If the capital cost could be kept down this electro-synthesis route has the potential for expanded use in the pulp and paper industry as an onsite source of peroxide.

In a previous communication [3] we described a novel perforated *bipole* trickle-bed electrochemical reactor for peroxide generation by electro-reduction of oxygen, aimed to reduce the high capital cost normally associated with this electro-synthesis. The reactor in that work had 1 to 2 cells, each with graphite felt (3D) cathodes

120 mm long by 25 mm wide by 3.2 mm thick, operated at current densities in the range 1–5 kA m^{-2}, ca. 800 kPa (abs) pressure and temperature (in/out) 20–45 °C. The reactants O_2 and NaOH were supplied in a co-current upflow mode in that operation. Conventional trickle bed reactors are operated in a co-current gas and liquid downflow mode. But a co-current gas liquid upflow mode was used in that work as both the mass transfer capacity and the liquid hold up were higher in this flow mode [4]. Increased liquid hold up increases the effective electrolyte conductivity which lowers the IR losses in the reactor. The reactor showed good performance (current efficiency ~78% at 2 kA m^{-2} and a specific energy of 5 kWh per kg of peroxide generated) with peroxide concentrations from 0.02 to 0.15 M in 1 M NaOH.

To have a commercial process at hand, it is desirable to increase the peroxide current efficiency at high current density and to scale-up the perforated bipole electrochemical reactor to industrial size.

Past work on scale-up of a trickle-bed electrochemical reactor for generating alkaline peroxide has been reported by Oloman [5], Yamada et al. [6, 7] and the Dow (H-D Tech) cell group [8, 9]. Oloman presented data on scale-up from a single 0.039 m^2 "one compartment" cell to a corresponding 5-cell bipolar reactor with particulate graphite cathodes and also to a single 0.5 m^2 cell operating at superficial current density of 0.5 kA m^{-2} with an electrolyte of 2 M NaOH. The scale-up of superficial area in a single cell was accompanied by a decrease in current efficiency attributed to dispersion and mal-distribution of fluids in the larger cell. Yamada et al. used a dual compartment single cell with a stainless steel web anode separated from a carbon felt cathode by a cation membrane. The poor results obtained in a cell with 0.8 m^2 superficial cathode area, relative to a cathode area of 0.005 m^2, were attributed to uneven distribution of liquid (electrolyte) in the cathode felt.

Yamada et al. also investigated the liquid and oxygen supply modes. It was seen from their work that when the liquid and the oxygen gas were supplied separately to the cathode, the current efficiency decreased compared to that for a uniformly mixed flow of liquid and oxygen gas obtained by 'spraying' the fluids into the cathode bed.

The Dow (H-D Tech) group scaled-up to a commercial multi-cell mono-polar reactor with superficial cathode area of ~1 m^2 per cell. This approach gave a product equivalent to about 1 M H_2O_2 in 1.5 M NaOH with peroxide current efficiency of 90% at a superficial current density of 0.62 kA m^{-2} and 2.0 V cell. The major limitation of this reactor was however, its low superficial current density and consequent high capital cost that has apparently (so far) restricted it to only one commercial application. Apart from the current density limitation the reactor was constrained by the electrolyte diaphragm-flow design to a maximum cell height of about 1 m.

The present work aims to address the issue of reactor scale-up at three levels:

(i) Increasing the superficial electrode area per cell in the multi-cell perforated bipole reactor of our previous communication [3].
(ii) Improving the uniformity of the 2-phase fluid flow in the cathode of the larger cells.
(iii) Changing from a micro-porous polypropylene separator to a polyethylene separator with improved transport properties, together with increasing the concentration of NaOH in the electrolyte from 1 to 2 M.

The theoretical level of reactor modeling will be described in a subsequent communication, aimed to shed light on the perforation parameters, and to show the comparison between the model and experimental results of this work.

2. Reactor concept

The multi-cell trickle-bed bipolar electrochemical reactor used here has porous diaphragm separators, with perforations in the bipole electrodes that let oxygen generated at each anode disengage from its surface into the adjacent cathode. Table 1 summarizes the reactions that occur here in the synthesis of alkaline peroxide, as detailed along with the reactor concept and configuration in our previous communication [3].

3. Experimental

Experiments were carried out on two reactors to see the effect of cathode size:

(1) Reactor-A (Cathode: 120 mm long by 25 mm wide and 3.2 mm thick.)
(2) Reactor-B (Cathode: 630 mm long by 40 mm wide and 3.2 mm thick.)

Both reactors A and B were operated in the one-cell and two-cell (bipolar) assemblies shown respectively in Figures 1 and 2.

Table 1. Reactions in electro-synthesis of alkaline peroxide

Reaction	E_e° V vs. NHE at 298 K (pH = 14)	
Cathode		
$O_2 + H_2O + 2e^- \Rightarrow OH^- + HO_2^-$	−0.076	1
$HO_2^- + H_2O + 2e^- \Rightarrow 3OH^-$	+ 0.878	2
$2H_2O + 2e^- \Rightarrow H_2 + 2OH^-$	−0.830	3
Anode		
$O_2 + 2H_2O + 4e^- \Leftarrow 4OH^-$	+ 0.401	4
$O_2 + H_2O + 2e^- \Leftarrow OH^- + HO_2^-$	−0.076	5
Bulk		
$2HO_2^- \Rightarrow 2OH^- + O_2$	–	6

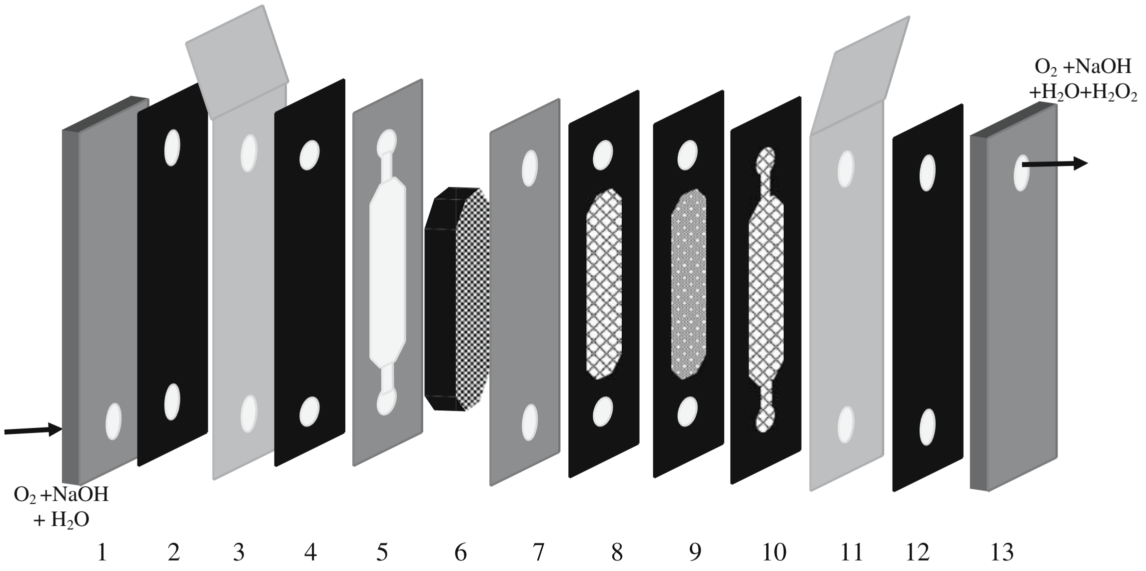

1, 13 - Carbon steel cell body
2, 5, 12 - Durabla gasket
4 - Grafoil sheet
9 - Perforated anode (Grafoil)
10 - Dummy anode (nickel mesh)
7 - Diaphragm (microporous polyalkene)
8 - Anode (nickel mesh)
3, 11 - S.S. current feeder
6 - Graphite felt (3.2 mm thick)

Fig. 1. One-cell reactor assembly.

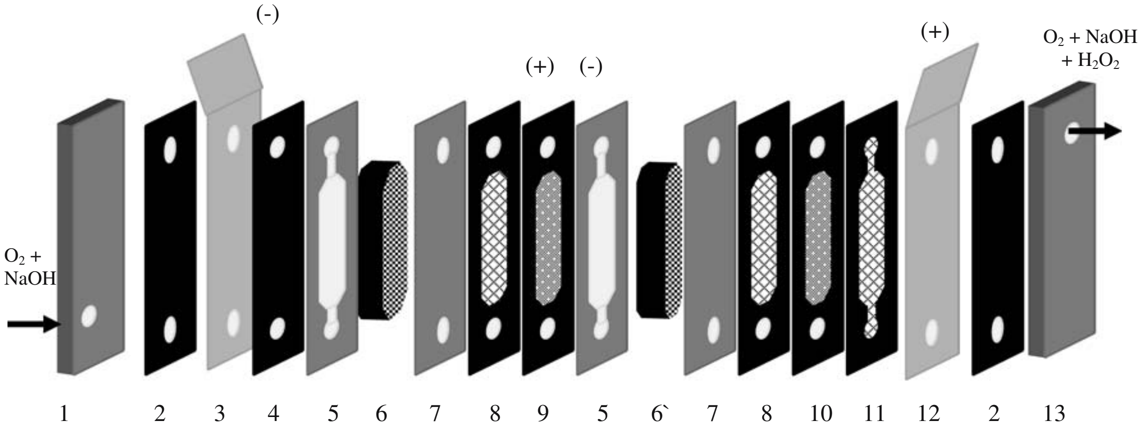

1, 13 - Carbon steel cell body
2, 5 - Durabla gasket
3, 12 - S.S. current feeder
4 - Grafoil sheet
6, 6` - Graphite felt (3.2 mm thick)
8 - Anode (nickel mesh)
9 - Perforated bipolar electrode (Grafoil)
10 - Perforated anode (Grafoil)
11 - Dummy anode (nickel mesh)
7 - Diaphragm (micro-porous polyalkene)

Fig. 2. Two-cell (bipolar) reactor assembly.

3.1. *Reactor components*

The properties of reactor components in Figures 1 and 2 are similar to those described in our previous communication [3]. For reactor-B the components have been slightly altered as described below:

3.1.1. *Anode*

The anode/bipole is a layered combination of plain nickel mesh (100 mesh inch^{-1} from Argus Inc. Virginia, USA) and perforated Grafoil[1] (1.6 mm thick, from Union Carbide Corp. New Jersey, USA). Nickel mesh is used in conjunction with Grafoil to enhance the surface area of the anode. This enhanced surface area helps to keep the anode wet at high current density and prevent localized Joule heating which could lead the diaphragm to burn-out. The loss of current efficiency due to current bypassing via the perforations is minimized by the right

---

[1] Grafoil is a compressed graphite sheet with stainless steel insert.

choice of the perforation parameters and compensated by the ability to operate the reactor at super-atmospheric pressure with (superficial) current densities up to about 6 kA m^{-2}. Previous work at U.B.C. [10, 11] found good results for 1.6 mm diameter perforations with 2% coverage and these values were used in the present work.

3.1.2. *Diaphragm*

The transport properties of the diaphragm separator (item 7 in Figure 1), are critical to the operation of the reactor in so far as they affect the cell voltage and the loss of peroxide by convection to the anode (reaction 5). Table 2 lists some properties of the two diaphragm materials used in the present work, namely microporous polypropylene (SCIMAT 700/20) and microporous polyethylene (SOLUPOR E075–9H06A).

3.1.3. *Cathode*

The properties of the graphite felts used for the cathode in reactors-A and B are listed in Table 3.

4. Scale-up philosophy

The philosophy of scaling-up chemical process units requires that values of corresponding dimensionless groups of the two units are similar [12]. Several similarity criteria have been defined to guide the engineer to scale-up a reactor [13]. The criteria normally employed in thermochemical reactors are those of geometric, kinematic and thermal similarity between the reactors. In the case of electrochemical reactors an additional criterion necessary to define the scale-up is that of current/potential similarity. These four criteria are discussed below:

4.1. *Geometric similarity*

Geometric similarity is achieved by fixing the dimensional ratios of the corresponding reactors. However, for electrochemical reactors, this criterion cannot normally be met, as increasing the inter-electrode gap would give a high voltage drop and increased energy costs. Further, in 3D electrodes an increased electrode thickness may cause a decrease in the average electric potential and/or promote secondary electrode reactions [14]. Therefore, geometric similarity is usually sacrificed in favor of current/potential similarity in electrochemical reactors. Scale-up in electrochemical reactors is achieved by using multiple cells and reactor units [15].

Table 2. Diaphragm properties

Source	Material	Type	Thickness mm	Poro-sity %	Basis weight g m^{-2}	Ion exchange capacity meq g m^{-1}	Mean Pore Size μm
SCIMAT Ltd. UK	Microporous polypropylene	700/20	0.15	na	45	0.6	na
SOLUPOR DSM Solutech, Netherlands	Microporous polyethylene	E075–9H06A	0.039	76	9	1.1	0.6

Table 3. Graphite felt properties Source: (Type Grade GF, Metaullics Systems Inc.)

Property	Value	Source
Initial porosity, ε_o	0.95	Metaullics systems Inc.
Mean fibre diameter (μm)	20	Idem
d_f Fibre density (kg m^{-3})	1500	Idem
Graphitization (°C h^{-1})	2400/2	Idem
Carbon content (%)	99	Idem
Uncompressed thickness (mm), t_o		
Reactor-A	6.4	Measured
Reactor-B	8.2	Measured
Compressed thickness (mm), t		
Reactor-A	3.2	Measured
Reactor-B	3.2	Measured
Compressed porosity, ε		$\varepsilon 1 - t_o(1 - \varepsilon_o)/t$
Reactor-A	0.90	
Reactor-B	0.87	
Compressed specific surface area (m^{-1}), s		$s = 4(1 - \varepsilon)/d_f$
Reactor-A	20000	
Reactor-B	26000	
Electronic conductivity of compressed matrix (S m^{-1}), k_{aps}		$k_{aps} = 10 + 2800(1 - \varepsilon/\varepsilon_o)^{1.55}$ [17]
Reactor-A	39.2	
Reactor-B	70.5	

4.2. *Kinematic similarity*

Kinematic similarity is concerned with the flow velocities within a system. In any continuous reactor, the gas and liquid flow loads, or more generally the Reynolds' numbers, govern the pressure drop, fluid hold-up and mass transfer capacity in the system [5]. Therefore it was desirable to maintain similar gas and liquid flow velocities through the corresponding reactors. In the present work, a liquid flow of 20–25 $cm^3\ min^{-1}$ per cell ($3.3–4.16 \times 10^{-7}\ m^3\ s^{-1}$) was used for reactor-A with a cell cross-sectional flow area of 3.2 mm by 25 mm i.e. 80 mm^2. The selection of liquid flow in reactor-A was based on past experience with the system. To maintain a similar velocity for the liquid flow in the reactor-B with a cell cross-sectional flow area of 3.2 mm by 40 mm (128 mm^2), a liquid flow in the range 32–40 $cm^3\ min^{-1}$ ($5.3–6.6 \times 10^{-7}\ m^3\ s^{-1}$) was indicated. The liquid flow rate used in the present work with reactor B was 40–45 $cm^3\ min^{-1}$ ($6.6–7.4 \times 10^{-7}\ m^3\ s^{-1}$).

The gas load in the scaled-up reactor was determined by an analogous similarity criterion but was also constrained by the stoichiometry of reaction 1. The oxygen flow rate in reactor-A was ca. 200 cm^3 (STP) min^{-1} ($3.3 \times 10^{-6}\ m^3\ s^{-1}$), whereas for reactor-B oxygen flow was in the range 300–420 cm^3 (STP)/min ($5–6.9 \times 10^{-6}\ m^3\ s^{-1}$).

4.3. *Thermal similarity*

Thermal similarity implies matching the temperatures in corresponding portions of the reactors under comparison. This condition may be approached by temperature control through internal heat transfer surfaces and/or heat exchange with recycling reactants. Thermal similarity is difficult to maintain in the scale-up of electrochemical reactors due to the effect of Joule heating within inter-electrode dimensions of the order of millimeters. The method of providing cooling channels between cells (as in conventional fuel cell stacks) is not practical in a perforated bipole reactor and in any case would defeat the purpose of the reactor design, which is to lower capital cost in the electro-synthesis of alkaline peroxide.

4.4. *Current/potential similarity*

Electrochemical reactors, unlike their thermochemical counterparts, require electrical similarity and this is usually the most important criterion in the scale-up of such reactors. Electrical similarity exists between two units when corresponding electrode potential and current density differences bear a constant ratio [15]. This criterion necessitates a constant inter-electrode gap on scale-up. One factor normally employed to quantify the effect is the Wagner number (*Wa*), which may be defined as:

$$Wa = \left(\frac{\kappa}{L}\right)\left(\frac{dV}{di}\right) \qquad (1)$$

where κ is the electrolyte conductivity, V the electrode potential, i the current density and L the characteristic length. For electrical similarity, the Wagner number in the two reactors should have the same value at all points being compared. In 3D electrodes, an inverse Wagner number qualitatively describes the current distribution in the system [16]. This sets the rules to get uniform current distribution for scale-up. i.e. for reactors operating under kinetic control, better uniformity is obtained for a higher slope of polarization curve, larger conductivity of electrolyte (κ in equation (1)), smaller characteristic length (*L* in the equation (1)) and lower average current density.

The constraints of current/potential similarity require that the scale-up of electrochemical reactors to industrial capacity is usually achieved by (i) fixing the inter-electrode gap while increasing the superficial area of individual cells (e.g. up to about 2 m^2/cell) and (ii) stacking individual cells in monopolar or bipolar multi-cell reactors (e.g. containing up to 200 cells).

Our approach to scaling-up the perforated bipole peroxide reactor was aimed to achieve the high current density (up to 5 kA m^{-2}) and efficiency reported previously [3] by fixing the cathode thickness and inter-electrode gap along with the liquid load, increasing the superficial area per cell, increasing gas load to match the current stoichiometry, unifying fluid distribution in the large cell and stacking more than one large cell in a bipolar reactor. While these steps met some of the conditions for scale-up, other conditions were violated as a result of:

- variation in composition, pressure and temperature along the cell (due to reactant conversion, flow resistance and Joule heating) that became greater with increased cell length.
- current/potential distribution through the perforations of the bipole stack.
- mal-distribution of fluid flow (gas and liquid) between cells in the bipole stack.

The above issues were exacerbated by the fact that the peroxide reactor uses a three-dimensional (3D) cathode in which fluid dispersion, mass transfer, potential, pressure and temperature gradients interact through the reaction kinetics to determine the peroxide current efficiency. These difficulties were partly resolved in complimentary theoretical work where reactors-A and-B were modeled both as single cells and as two-cell bipole stacks. This modeling work will be presented in a subsequent communication.

4.5. *Gas and liquid distribution*

The effective operation of a trickle-bed electrode requires uniform distribution of gas (reactant) and liquid (electrolyte) over the surface of the solid (electrode). In this respect gas and liquid flow distribution is a major issue in the scale-up of trickle bed electrochemical reactors.

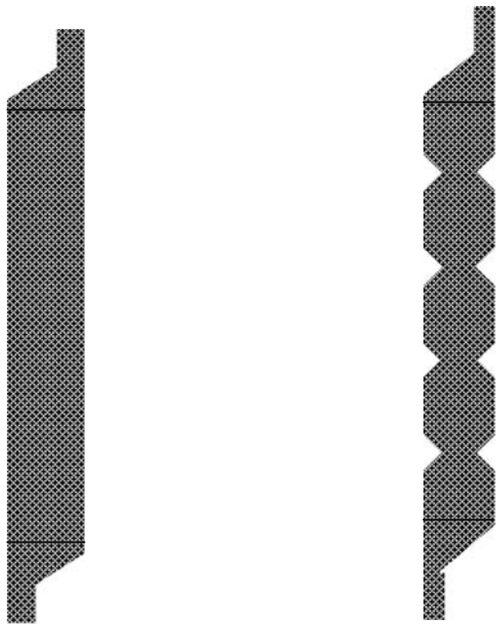

a. U n-constricted cathode **b.** Constricted cathode

Fig. 3. Cathode shapes.

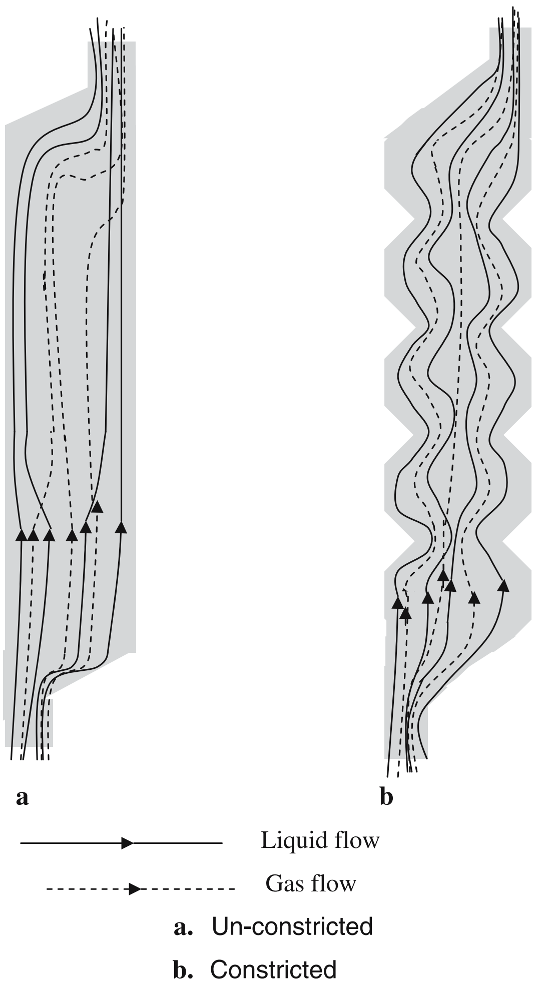

Fig. 5. Flow distribution of gas and liquid through graphite felt cathodes.

To assist the scale-up the flow was visualized in transparent mock-ups of the cathode beds of reactors-A and-B, made by bolting the gasketed graphite felt between two Perspex sheets and operated with two-phase (G/L) upward flow at 20 °C with inlet/outlet pressure of 225/101 kPa(abs). In reactor-A the gas and liquid passed through the un-constricted graphite felt in slug flow. i.e. slugs of liquid were observed to flow through the felt with gas flowing intermittently between the slugs. The liquid slugs moved uniformly throughout the length (120 mm) of reactor and covered the entire width (25 mm).

The transparent (Perspex) version of reactor-B used the same liquid load as reactor-A but an increased gas load to account for the higher oxygen consumption in the longer reactor. For 1.25 times the stoichiometric requirement at 5 kA m^{-2} (maximum used in the present work) the gas (oxygen) feed flow in reactor-B is 420 cm^3(STP) min^{-1} per cell. While reactor-B was intended to operate with an inlet/outlet pressure of 900/800 kPa(abs) the Perspex model could withstand only up to 225 kPa(abs), thus the oxygen flow used in the visualization test to match the gas velocity in reactor-B was from 50 to 200 cm^3 (STP)/min (i.e. 8×10^{-7} to 3×10^{-6} m^3 s^{-1}).

When the un-constricted graphite felt of Figure 3 was used in the Perspex version of reactor-B, with gas and liquid flows respectively 50 cm^3(STP) min^{-1} and 40 cm^3 min^{-1} for a feed pressure 225 kPa(abs), it was observed that at approximately 1/5th of the cell length above the inlet the gas and liquid flows became segregated as shown schematically in Figure 5a. At this region the gas (oxygen) began flowing through the centre and the liquid (electrolyte) along the edges of the

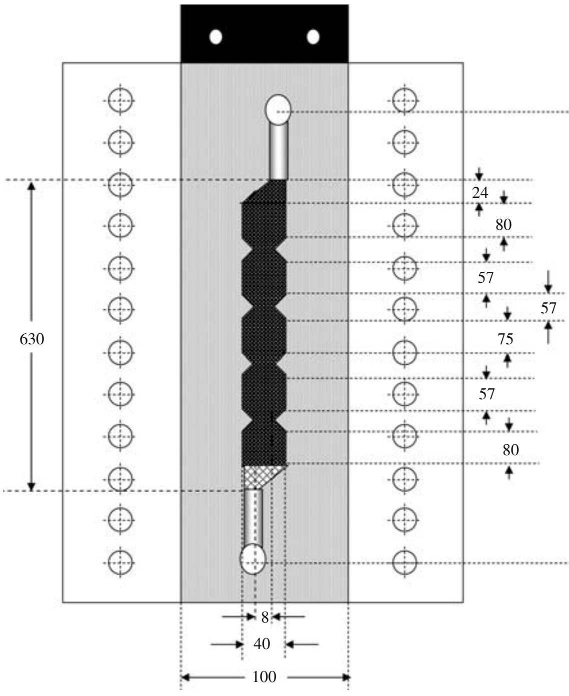

Fig. 4. Constricted cathode dimensions (in mm).

graphite felt. This flow separation led to poor contacting between the three phases (gas–liquid–solid).

After several trials using different constricted cathode configurations the constricted cathode in Figure 4 was arrived at and it was found that these constrictions promoted the re-distribution of gas and liquid and maintained relatively good three-phase contacting in the graphite felt bed. Both the un-constricted and constricted cathodes (Figure 5a and 5b) were used in the subsequent tests of reactor-B.

5. Results and discussion

Figures 6 and 7 show the results of experiments for peroxide current efficiency and peroxide concentration on a one-cell reactor-A compared to a one-cell reactor-B with both un-constricted and constricted cathodes. These experiments were done under the conditions listed in Table 4.

Figure 6 shows that the current efficiencies in reactor-B with the un-constricted cathode are substantially lower than those with the constricted cathode operating at essentially the same conditions. At 5 kA m^{-2}, the peroxide current efficiency for the un-constricted cathode is 27% compared to 57% for the constricted cathode. This significant gain in peroxide current efficiency was due to a more even flow distribution of gas and electrolyte through the constricted cathode, with consequent better gas-liquid-solid contacting, compared to the un-constricted cathode. Figure 6 also shows that at 1 kA m^{-2} the current efficiency for reactor-A was much higher than the corresponding efficiency for the constricted reactor-B (85% vs. 63%). However the efficiencies approach similar values at current densities of 3–5 kA m^{-2} (69–65% for reactor-A and 65–57% for reactor-B). As the current efficiencies in reactor-A and-B were similar at current density exceeding 3 kA m^{-2}, the constricted reactor-B was taken as a scaled-up version of the one-cell reactor for the purpose of this work.

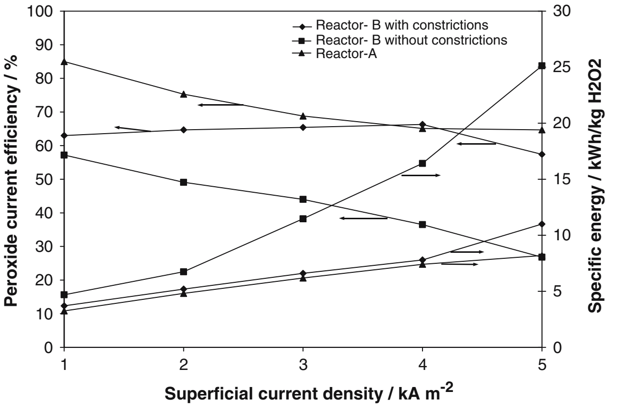

Fig. 6. Peroxide current efficiency and specific energy for one-cell reactors A and B using polypropylene diaphragms with un-constricted and constricted cathodes (other conditions as in Table 4).

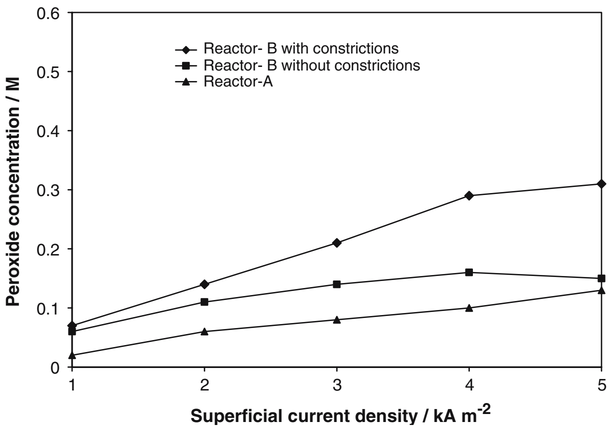

Fig. 7. Peroxide concentration for one-cell reactors A and B using polypropylene diaphragms, with un-constricted and constricted cathodes (other conditions as in Table 4).

Even though reactor-A was scaled-up to the one-cell constricted reactor-B, the peroxide current efficiencies in reactor-B were too low for the process to be economically viable. The low current efficiencies were a result of a high peroxide loss through the diaphragm. Peroxide loss through the diaphragm occurs by convection, diffusion and migration of perhydroxyl ions that are subsequently oxidized at the anode. The convective loss, which is the major of these losses, was lowered by replacing the polypropylene diaphragm (SCIMAT 700/20) with a polyethylene diaphragm (SOLUPOR-EH06A) that has a different set of transport properties, as shown in Table 2.

Figure 8 shows the peroxide current efficiency and specific energy in the one-cell constricted reactor-B with both polypropylene and polyethylene diaphragms, using electrolytes of 1 and 2 M NaOH. At 1 kA m^{-2} in 1 M NaOH the current efficiencies with the polypropylene and polyethylene diaphragms were respectively 63% and 95%. Increasing the current density to 5 kA m^{-2} in 1 M NaOH dropped the current efficiency with the polyethylene diaphragm to 63%, but changing the electrolyte from 1 to 2 M NaOH raised the corresponding current efficiency to 80%. Also, as shown in Figure 9, the highest peroxide concentration from the one-cell constricted reactor-B with a polyethylene diaphragm at 5 kA m^{-2} increased from 0.44 M in 1 M NaOH to 0.57 M in 2 M NaOH.

The drop in peroxide current efficiency at high current density in 1 M NaOH was probably due to the oxygen mass transfer constraint on the cathode-coupled to the conductivity of 1 M NaOH and electro-active cathode thickness. Raising the NaOH concentration to 2 M increased the electro-active thickness of the cathode, thus lowering the real current density and increasing the current efficiency for peroxide generation. Another reason for the drop in peroxide current efficiency in 1 M NaOH could be that the primary anode reaction (reaction 4) became OH^- mass transport limited at high current density (e.g. 5 kA m^{-2}), with a subsequent

Table 4. Experimental conditions

Experiment →		Figure 5, 6 Reactor-A	Figure5, 6 Reactor-B	Figures 7, 8 Reactor-B	Figures 9, 10 Reactor-A	Figures 9, 10 Reactor-B
NaOH conc.	M	1.0	1.0–2.0	1.0–2.0	1.0	1.0–2.0
NaOH flow	ml/min/cell	20–25	55	45–55	20–25	45–55
O_2 flow	ml STP/min/cell	200	300	300	200	300
Reactor pressure	kPa (abs) in–out	900-875	900–600	900–600	900–875	900–600
Reactor Temperature	°C in–out	20–45 °C	20–75 °C	20–75 °C	20–45 °C	20–75 °C
Anode		Ni 100$^{\#}$ + Grafoil	Ni 100$^{\#}$ + Grafoil	Ni 100$^{\#}$ + Grafoil	Ni 100$^{\#}$ + Grafoil	Ni 100$^{\#}$ + Grafoil
Perforation	diam mm/ coverage %	1.6/2	1.6/2	1.6/2	1.6/2	1.6/2
Diaphragm type		SCIMAT 700/20	SCIMAT 700/20	SCIMAT 700/20 or SOLUPOR EH06A	SCIMAT 700/20	SCIMAT 700/20 or SOLUPOR EH06A
Cathode: Graphite felt	Thickness mm/porosity %	3.2/90	3.2/87	3.2/87	3.2/90	3.2/87
No. of cells		1	1	1	2	2

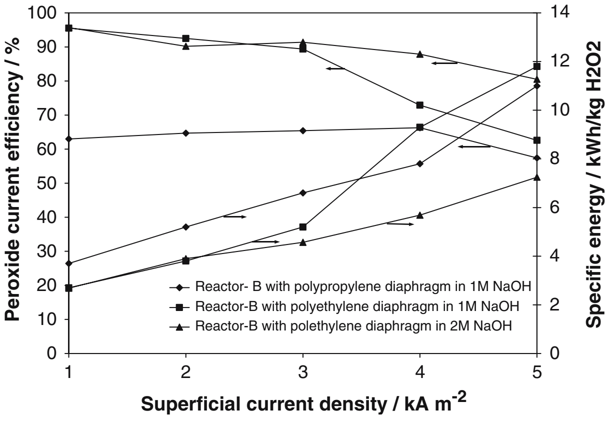

Fig. 8. Peroxide current efficiency and specific energy in a one-cell constricted reactor-B with polyethylene and polypropylene diaphragms (other conditions as in Table 4).

increase in the rate of the competitive electro-oxidation of HO_2^- (reaction 5). In 2 M NaOH the balance of reactions 4 and 5 may be more favorable for the preservation of the peroxide.

Experiments were also conducted on the two-cell bipolar reactors-A and-B to see the effect of scale-up using polyethylene and polypropylene diaphragms in 1 and 2 M NaOH, with the results given in Figures 10 and 11. Figure 10 shows that the peroxide current efficiencies and specific energy consumptions from 2–4 kA m^{-2} were nearly the same in the two-cell reactors-A and-B with polypropylene diaphragms. Therefore the two-cell constricted reactor-B was taken as a scaled-up version of the 2-cell reactor-A.

Figure 10 further shows that the peroxide current efficiency in the two-cell constricted reactor-B can be increased by using a polyethylene diaphragm with 2 M NaOH, as was seen in the single-cell experiments. The current efficiency and peroxide concentration at 3 kA m^{-2} in the two-cell constricted reactor-B, using the polyethylene diaphragm and 2 M NaOH, reached respectively 84% and 0.42 M, while the specific electrical energy consumption for peroxide fell to 4.1 kWh per kg of H_2O_2. The corresponding values at 5 kA m^{-2} were 74% current efficiency with 0.6 M peroxide in 2 M NaOH and specific energy 6.4 kWh per kg H_2O_2.

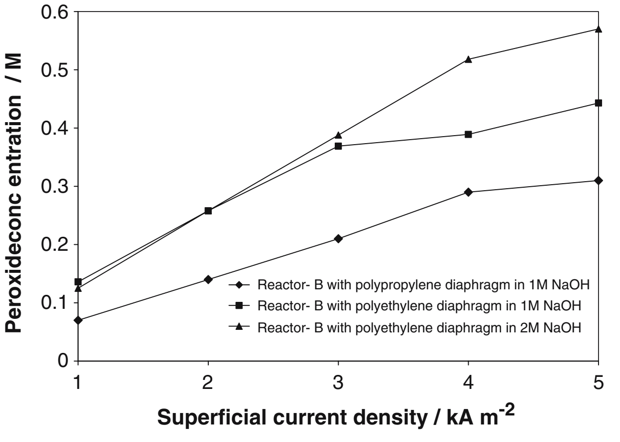

Fig. 9. Peroxide concentration in a one-cell constricted reactor-B with polyethylene and polypropylene diaphragms (other conditions as in Table 4).

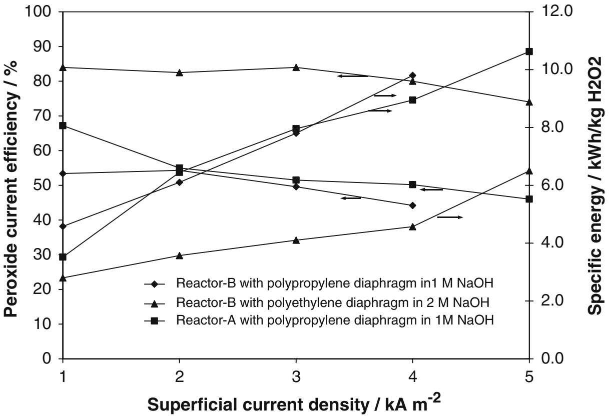

Fig. 10. Peroxide current efficiency and specific energy in two-cell reactors-A and–B (constricted) with polyethylene and polypropylene diaphragms (other conditions as in Table 4).

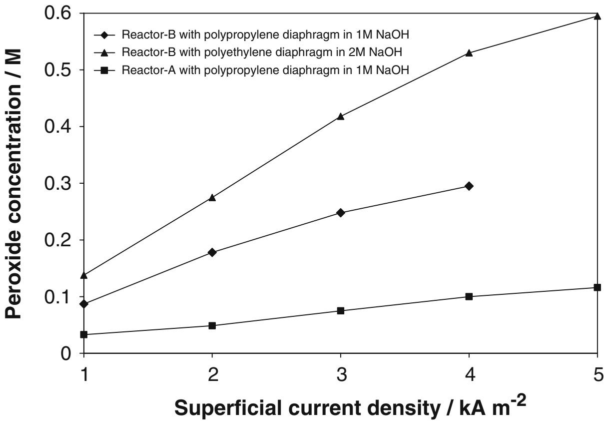

Fig. 11. Peroxide concentration in two-cell reactors-A and B (constricted) with polyethylene and polypropylene diaphragms (other conditions as in Table 4).

6. Conclusions

The perforated bipole trickle-bed electrochemical reactor of our previous communication [3] was scaled-up from cathode dimensions 120 mm high by 25 mm wide, and 3.2 mm thick (reactor-A) to 630 mm high by 40 mm wide and 3.2 mm thick (reactor-B). The scale-up was achieved by the introduction of constrictions that prevent segregation of the 2-phase flow in the larger cell, combined with switching from a polypropylene to a polyethylene diaphragm with improved transport properties that suppress the electro-oxidation of accumulated peroxide. Experimental results show substantial improvement in the performance of reactor-B due to the presence of constrictions, the switch to a polyethylene diaphragm and an increase in the electrolyte feed concentration from 1 to 2 M NaOH.

In operation with feed conditions 900 kPa(abs)/20 °C at 5 kA m^{-2} the one-cell (monopolar) reactor-A with the polypropylene diaphragm generated 0.12 M peroxide in 1 M NaOH at 45 °C with a peroxide current efficiency of 66% and specific energy consumption 7.8 kWh per kg H_2O_2. Corresponding results for the two-cell (bipolar) constricted reactor-B with polyethylene diaphragms at 5 kA m^{-2} were 0.6 M peroxide in 2 M NaOH at 75 °C with current efficiency 74% and specific energy 6.4 kWh per kg H_2O_2. Further work is required to scale-up this bipolar reactor for more than two cells and superficial active area up to 1 m^2/cell.

Modeling the perforated bipole trickle-bed electrochemical reactor will be described in a subsequent communication, along with an outline of the process economics associated with the potential application of this novel unit to the electro-synthesis of alkaline peroxide solutions.

Acknowledgements

This work was supported by grants from the Government of Canada through the Natural Science and Engineering Research Council (NSERC) and the "Wood Pulps" Network of Centre of Excellence, with facilities supplied by the University of British Columbia (U.B.C.) and the U.B.C. Pulp and Paper Centre.

References

1. J.I. Kroschwitz *et al.*, *Kirk-Othmer Encyclopedia of Chemical Technology* (John Wiley & Sons, New York, 1999).
2. I.R. Mathur and R. Dawe, *TAPPI J* **82** (1999) 157.
3. N. Gupta and C. Oloman, *J. Appl. Electrochem.* **36**(2) (2006) 255.
4. I. Hodgson and C. Oloman, *Chem. Eng. Sci.* **54** (1999) 5777.
5. C. Oloman, *J. Electrochem. Soc.* **126**(11) (1979) 1885.
6. N. Yamada, T. Yaguchi and M. Sudoh, in *Advances in Mathematical Modelling and Simulation on Electrochemical Processes and Oxygen Depolarized Cathodes for Chlor-Alkali and Chlorate Processes* PV 98–10 (Electrochemical Society Proceedings Series, Pennington, NJ, 1998), p. 275.
7. N. Yamada, T. Yaguchi and M. Sudoh, *J. Electrochem. Soc.* **7** (1999) 2758.
8. A. Clifford, D. Dong, E. Giziewicz and D. Rogers, in C.W. Walton, John Van Zee and R.D. Varjian (Eds), 'Electrochemical Engineering and Small Scale Electrolytic Processing', PV 90–10 (The Electrochemical Society Proceedings Series, Pennington, NJ, 1990), p. 259.
9. J.A. McIntyre and R.F. Phillips, *J. Electrochem. Soc. Interface* **4**(1) (1995) 29.
10. C. Oloman, U.S. Pat. 4,728,409 (1988).
11. N. Gupta, 'Scale-up of the perforated bipole trickle-bed electrochemical reactor for the generation of alkaline peroxide' Ph.D.Thesis, University of British Columbia, Vancouver B.C. Canada (2004).
12. R.H. Perry and C.H. Chilton, *Chemical Engineers Handbook*, 5th ed., (McGraw Hill, New York, 1973).
13. H. Rase, *Chemical Reactor Design for Process Plants* (Wiley-Interscience, New York, 1977).
14. D. Pletcher and F. Walsh, *Industrial Electrochemistry* (Chapman and Hall, 1990).
15. F. Goodridge and K Scott, *Electrochemical Process Engineering* (Plenum Press, New York, 1994).
16. G. Prentice, *Electrochemical Engineering Principles* (Prentice Hall, 1991).
17. C. Oloman, M. Matte and C. Lum, *J. Electrochem. Soc.* **8** (1991) 2330.